Automated workflow for MR-PET attenuation correction in a tri-modality system using Dixon fat-water imaging based tissue classification

Dattesh D Shanbhag[1], Sheshadri Thiruvenkadam[1], Sandeep Kaushik[1], Rakesh Mullick[2], Scott D Wollenweber[3], and Florian Wiesinger[4]

[1]Medical Image Analysis Laboratory, GE Global Research, Bangalore, Karnataka, India, [2]GE Global Research, Biosignatures & Signal Processing, Bangalore, Karnataka, India, [3]GE Healthcare, PET Clinical Science, Waukesha, WI, United States, [4]Diagnostics & Biomedical Tech Laboratory, GE Global Research, Garching b. Munchen, Germany

Introduction: In the last few years, significant technical advancements have enabled integrated PET and MR imaging solutions. Both hybrid scanners (with simultaneous PET and MR image acquisition) as well as sequential systems (consisting of two separate scanners integrated by a dedicated patient transporter system) have been described and are becoming commercially available. MR-based PET attenuation correction (AC) is prerequisite for quantitative PET and hence a key determining factor for the success of PET/MR. Because the MR signal itself doesn't correlate with PET photon attenuation, MR image processing methods in form of atlas/template registration [1] and image segmentation [2] have been investigated. In this work, we present an automated workflow for whole body MR-based AC consisting of following steps: **i)** MR body contour segmentation, **ii)** MR auto-station identification, **iii)** lung segmentation, **iv)** fat-water separation, and **v)** auto-stitching of the single station segmented MR images towards a whole body MR-derived PET attenuation map. The method is shown to provide fast and robust tissue segmentation in presence of $B_{0/1}$induced signal variations and presence of noise. The method is currently evaluated on patients using an integrated, PET/CT + MR imaging setup, which warrants accurate tri-modality co-registration and allows direct comparison with gold-standard CT-based AC.

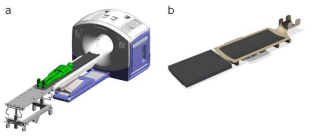

Figure 1: 3D schematic of axial, front-loading Transmobile patient transporter docked to the PET/CT table. b) Patient elevation board enabling handling of dedicated RF surface coils

Methods and Materials: **Trimodality system:** The tri-modality PET/CT+MR imaging setup consists of a time-of-flight Discovery PET/CT 690 scanner and a 3T Discovery MR750 scanner (both GE Healthcare, Waukesha, WI). The two scanners were installed in neighboring rooms and are connected via an MR compatible patient transporter system (Transmobile, Marquet Inc, Wayne, NJ) adapted as described in [**PatRef**]. This transporter system includes a shuttle which can be flexibly attached to both the PET/CT and the MR scanner and a transfer board for sliding the patient between the scanner table and the connected shuttle (Fig.1). For reproducible positioning on the PET/CT and the MR scanner the transfer board is laterally rail-guided and can be interlocked with the scanner tables in axial direction. An additional patient elevation board is used in between the transfer board and the patient, which allows flexible placement and removal of RF surface coils without repositioning of the patient. **Patient database:** The database for our study consisted of 6 patients. Following standardized injection of 350MBq of FDG and 60min uptake time, imaging started with multi-station, whole-body PET/CT scanning. Subsequently multi-station, whole-body MR imaging was performed using a dual-echo spoiled gradient echo sequence (LAVA-Flex) with TR=4ms, FA=15°, TE_1=1.15ms, TE_2=2.3ms, FOV=480x0.7*480x177mm^3, matrix=300x210x104pts, and 104 slices of 6.8mm thickness, resulting in 6-8 bed positions for head to pelvic floor coverage. From the obtained MR images, in-phase (I_{in}), out-phase, water (I_w) and fat (I_f) images were reconstructed using DIXON/IDEAL processing. The multi-station data was stitched using the overlap information between multi-station data. **Body Mask Generation:** Next, the body contour is generated for the whole-body stitched data to provide the background. We use a 2-class phase field formulation [Eq.1] to segment out the body mask for a given dataset [3, 4]. In Eq.[1], I is a weighted sum of signal intensity and image gradients from I_{in}, I_w and I_f data. The two-class function is represented by term "u", with u = 0 representing the background and u=1 the tissue. Parameters α, β, λ relate to noise variance, smoothness and sensitivity and are manually set. The Euler lagrange equation of Eq.[1] is a linear PDE and we minimize the energy using descent. The descent equation is solved using a semi implicit iterative method in a multi resolution framework. **Anatomy localization:** Using the whole body mask, range of slices approximately corresponding to shoulder, bottom of the lungs, pelvis and legs are identified. **Lung Segmentation:** The formulation for lung segmentation is similar to Eq.[1] (for a different set of parameters α, β, λ), with the indicator function being reversed so that u = 0 represents the tissue and u = 1 represents the lungs. The initial contour for lung segmentation is the body mask. **Fat/Water Classification:** For fat segmentation, the intra-body air statistics are estimated using the segmented lung region and background air region image values. A reliable threshold is set on the estimated range to remove air component from fat channel to obtain a coarse estimate of fat – I_{fl}. The fat fraction image is obtained as $I_{ffr} = (I_f / I_{in})$. The fat component is obtained as $I_{fe} = (I_{ffr} \geq 0.5) \cap I_{fl}$. Body region other than fat and lungs are considered as the water-tissue region. **MR-CT Registration:** A two-pass registration was performed using a constrained affine transform followed by quaternion transform driven by mutual information metric. The registration software reported the 3-parameter translational out-put and three parameter normalized quaternion. **4-Class CTAC and PET/MR AC:** CT attenuation maps were calculated by labeling the CT images into four classes (air/lung/fat/tissue) using the following attenuation value threshold window: Background/ Air: 0 mm^{-1}, Lungs: 0.0018 mm^{-1}, Fat: 0.0086 mm^{-1} and Water: 0.01 mm^{-1}. For MR images, above mentioned attenuation values were assigned to the tissue labels obtained from segmentation of fat/water images. For comparison with CT based AC, the LAVA-Flex water channel images were registered to CT data. Images were visually assessed for the degree of similarity and qualitative evaluation of the two AC techniques, while a quantitative evaluation is in progress. The workflow was implemented using the functionality available in the Insight Toolkit (registration, segmentation and fat/water classification) and Python (stitching and organ localization) [5, 6].

$$E[u] = \int_\Omega (1-u)^2 (I - c_{air})^2 dx + \int_\Omega u^2 \frac{\alpha}{1+\beta(I-c_{air})^2} dx + \tilde{\lambda} \int_\Omega u^2 (1-u)^2 dx + \lambda \int_\Omega |\nabla u|^2 dx \quad \textbf{Eq. [1]}$$

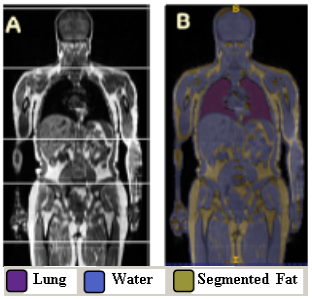

Figure 3 (a) Stitched whole body in-phase image with anatomy localization; (b) 4-class segmented MR image

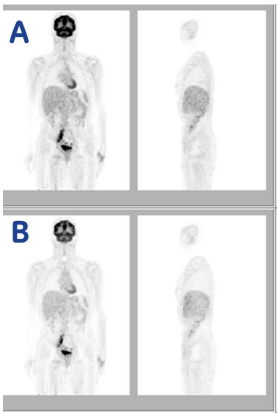

Figure 4 PET attenuation obtained from 4-class CT-AC (row: A), did not show significant differences compared to those obtained using MR-based AC (Row: B).

Results and Discussion: The mean lateral registration inaccuracy between PET and CT images was 1.8 mm ± 1.1 mm (torso) and 0.3 mm ± 2.2 mm (head/neck). Between PET and MR images registration inaccuracy was 0.7 mm ± 3.4 mm (torso) and 1.4 mm ± 4.3 (head/neck). Thus the tri-modality imaging setup with accurate co-registration (< 4 mm lateral misalignment between CT, PET and MR data sets) together with the short time span (<1h) between the sequential PET/CT and the MR measurements provides an ideal setup for the evaluation of MR-based AC methods versus gold standard CT-based AC. Fig. 2 demonstrates the robust segmentation provided by multi-scale, multi-channel phase-field based approach in presence of noise and weak signal intensity. The use of gradients helps deal with weak boundary and helps in classification of metal induced artifacts. The reliable identification of body contour provides robust organ localization and provides good initial estimate for lung, body air and fat/water segmentation (Fig. 3). Use of organ localization information allows to: (a).Optimize segmentation parameters for lung and body air segmentation (b) Provide distinction between lungs and other air-pockets in the body (c) Refine the body mask in regions of legs. Compared to previous approaches, use of lung and air-pockets to provide the lower threshold limit for defining the fat/water estimates results in reducing the amount of misplaced fat/water estimates and good correlation with CT. Visual comparison of four class CT-based AC versus MR-based AC reconstructed PET images did not indicate significant differences, demonstrating the validity of 4-class segmented MR-based AC (Fig. 4).

Conclusions: We have demonstrated an automated workflow for generation of the attenuation map for body Dixon-based MRI for PET attenuation correction. The use of a tri-modality system with dedicated patient transporter results in minimal degree of motion between PET-CT and MRI scans and improves the validation accuracy of AC of MR-PET system with gold standard PET-CT system.

References: [1]. Hoffman et.al. J Nucl Med 2008; 49:1875–1883 [2]. Martinez-Möller et.al. J Nucl Med 2009; 50:520–526 [3]. Samson et al. PAMI, v. 22(5), May 2000 [4]. Thiruvenkadam et.al. ICIP 2006 ; [5] http://www.itk.org. [6] http://www.python.org [PatRef]: [Calderon PD, et al, US Patent 7,467,004 B2].